Science Advances
AAAS

Supplementary Materials for

Diversification of the ruminant skull along an evolutionary line of least resistance

Daniel P. Rhoda *et al.*

Corresponding author: Daniel P. Rhoda, drhoda6@gmail.com

Sci. Adv. **9**, eade8929 (2023)
DOI: 10.1126/sciadv.ade8929

This PDF file includes:

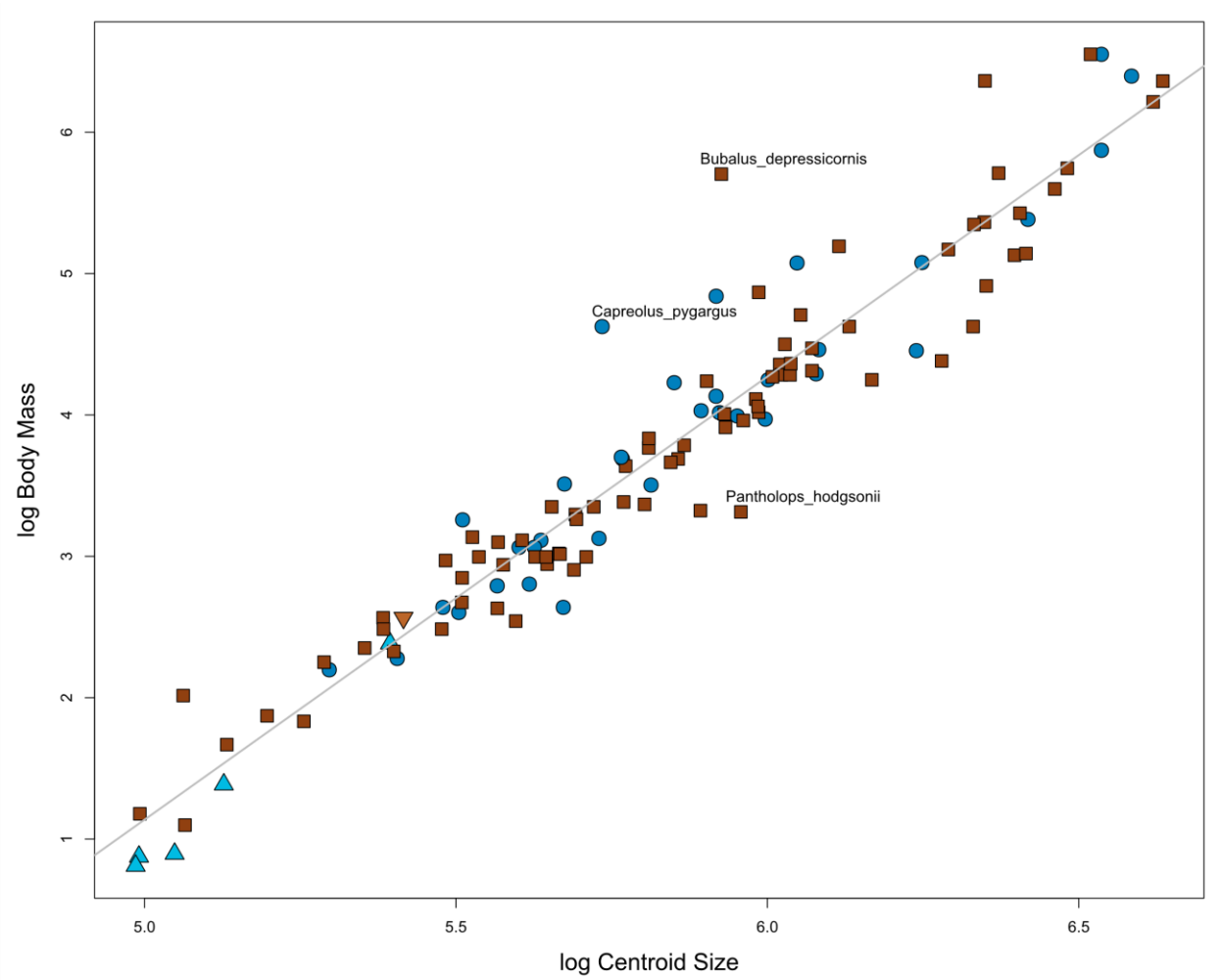

Fig. S1.
Linear regression analysis of log-transformed centroid size and log-transformed body mass. Note the very strong positive correlation (R^2 = 0.921). Species farthest away from the linear regression are labeled.

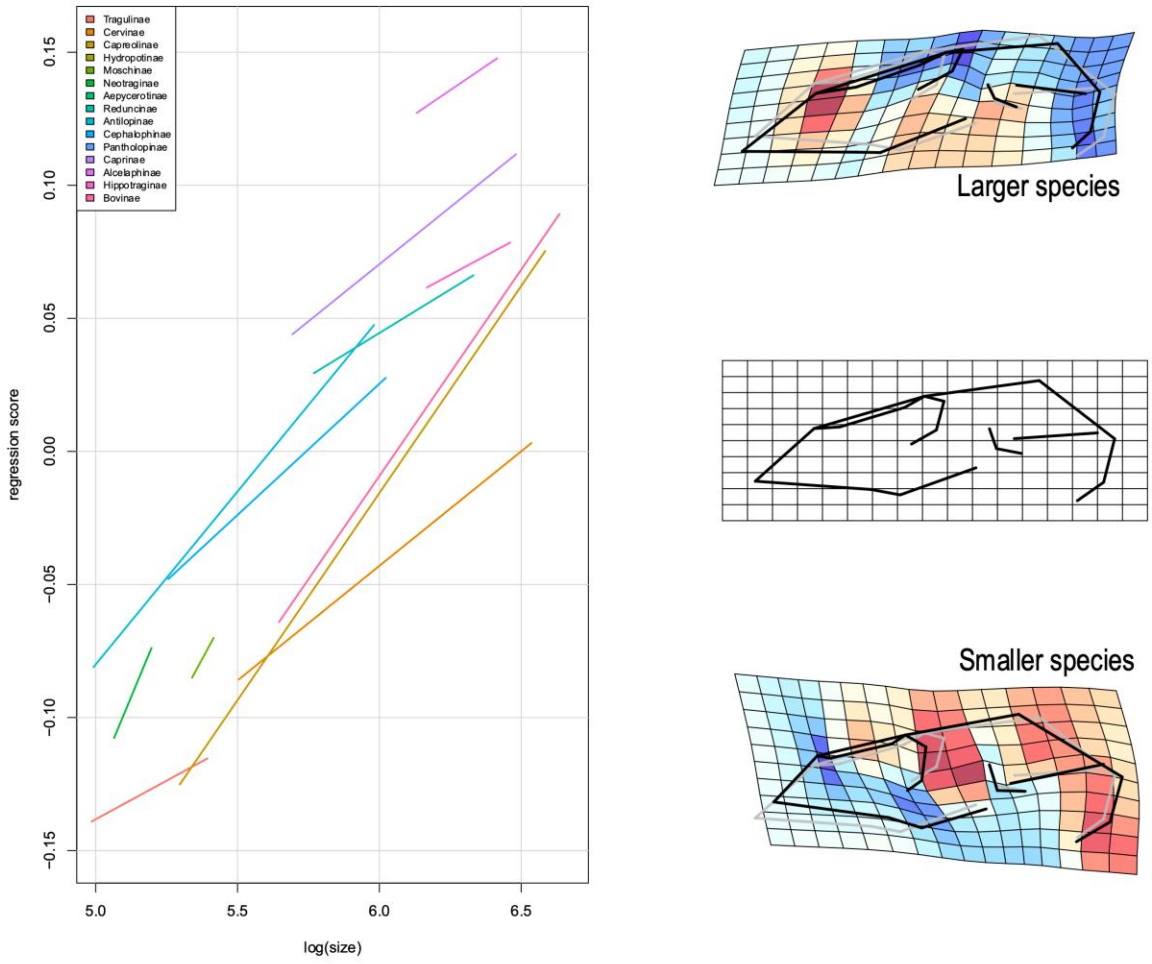

Fig. S2.

Homogeneity of slopes test of interspecific allometry in the ruminant skull. Allometric trajectory differed significantly by subfamily, but in each subfamily larger species have proportionally longer faces.

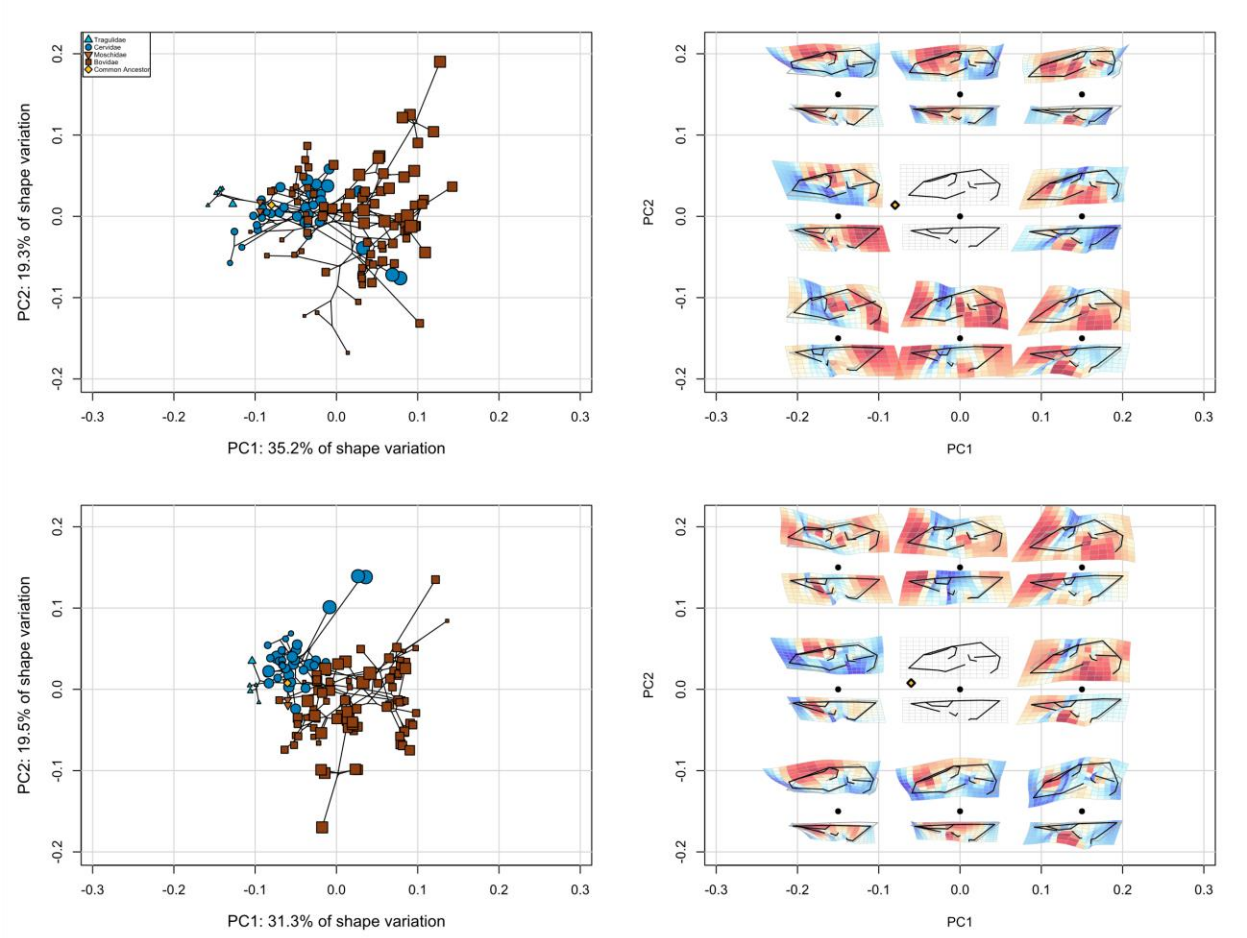

Fig. S3.

PCA morphospace with the raw data (top row) and with evolutionary allometry removed (bottom row). Shape variation across the morphospaces is presented in the right column. An interactive dashboard is available to visualize these different ordinations (https://danielrhoda.shinyapps.io/Ruminant_Dashboard/).

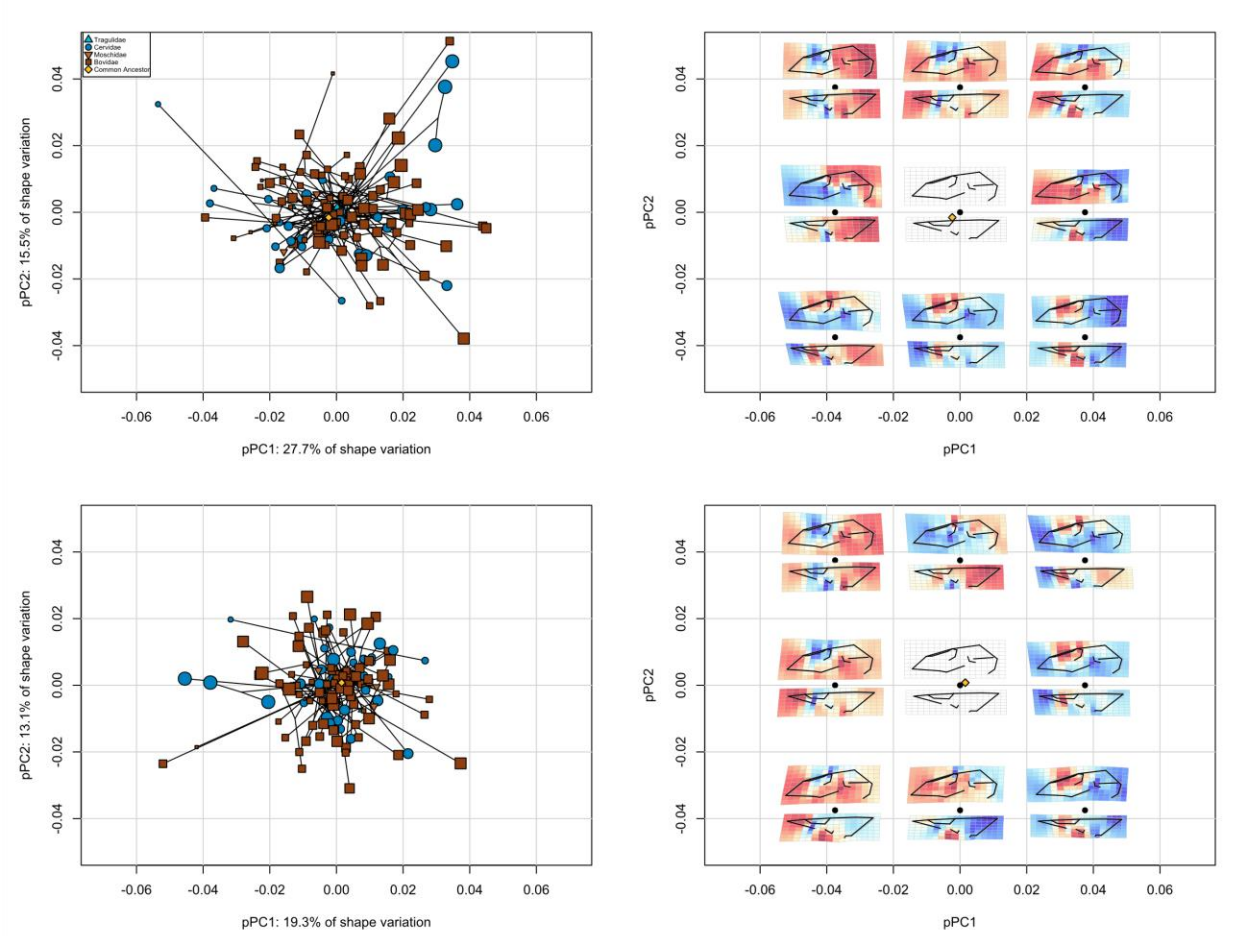

Fig. S4.

pPCA morphospace with the raw data (top row) and with evolutionary allometry removed (bottom row). Shape variation across the morphospaces is presented in the right column. An interactive dashboard is available to visualize these different ordinations (https://danielrhoda.shinyapps.io/Ruminant_Dashboard/).

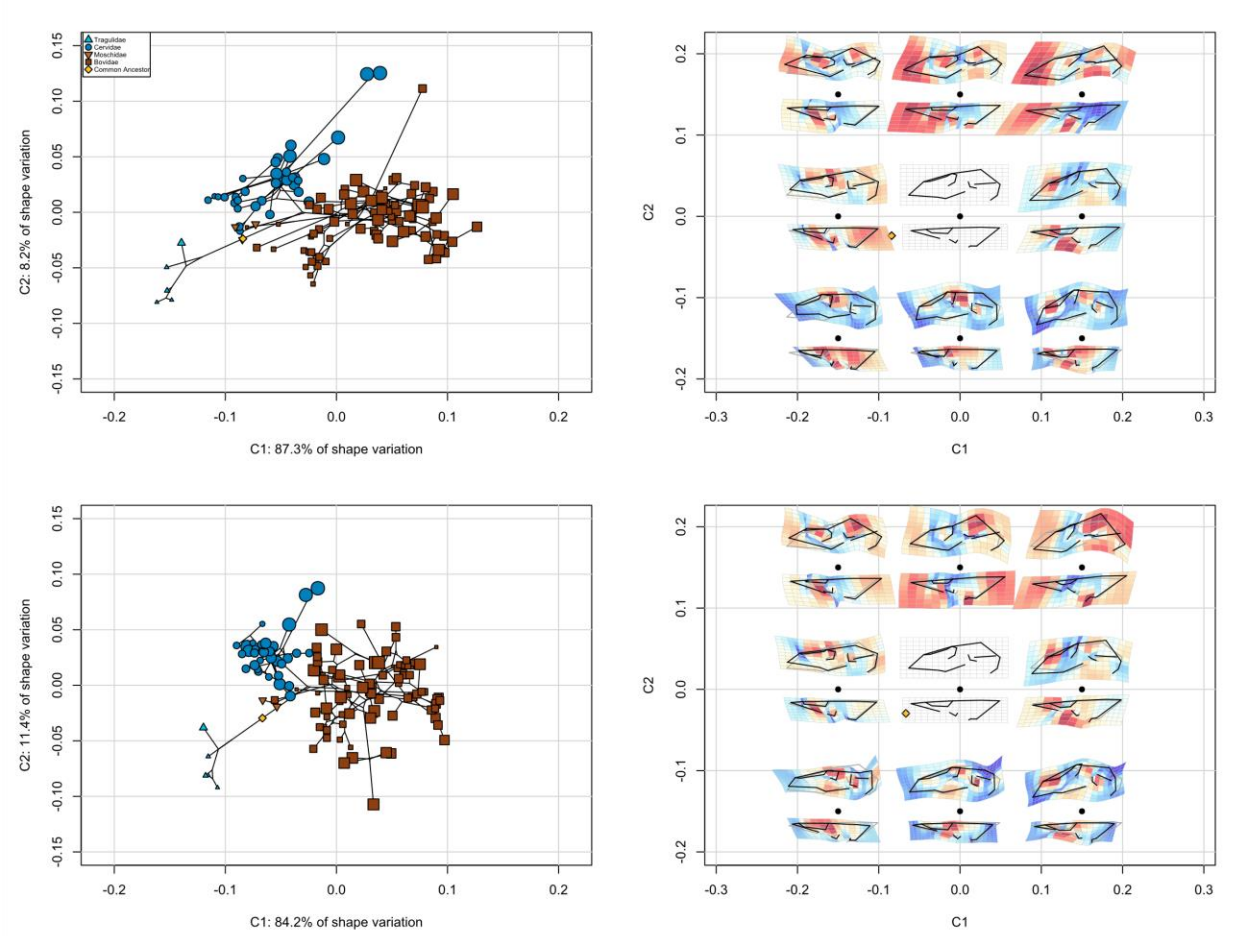

Fig. S5.

Phylogenetically-aligned components analysis morphospace with the raw data (top row) and with evolutionary allometry removed (bottom row). Shape variation across the morphospaces is presented in the right column. An interactive dashboard is available to visualize these different ordinations (https://danielrhoda.shinyapps.io/Ruminant_Dashboard/).

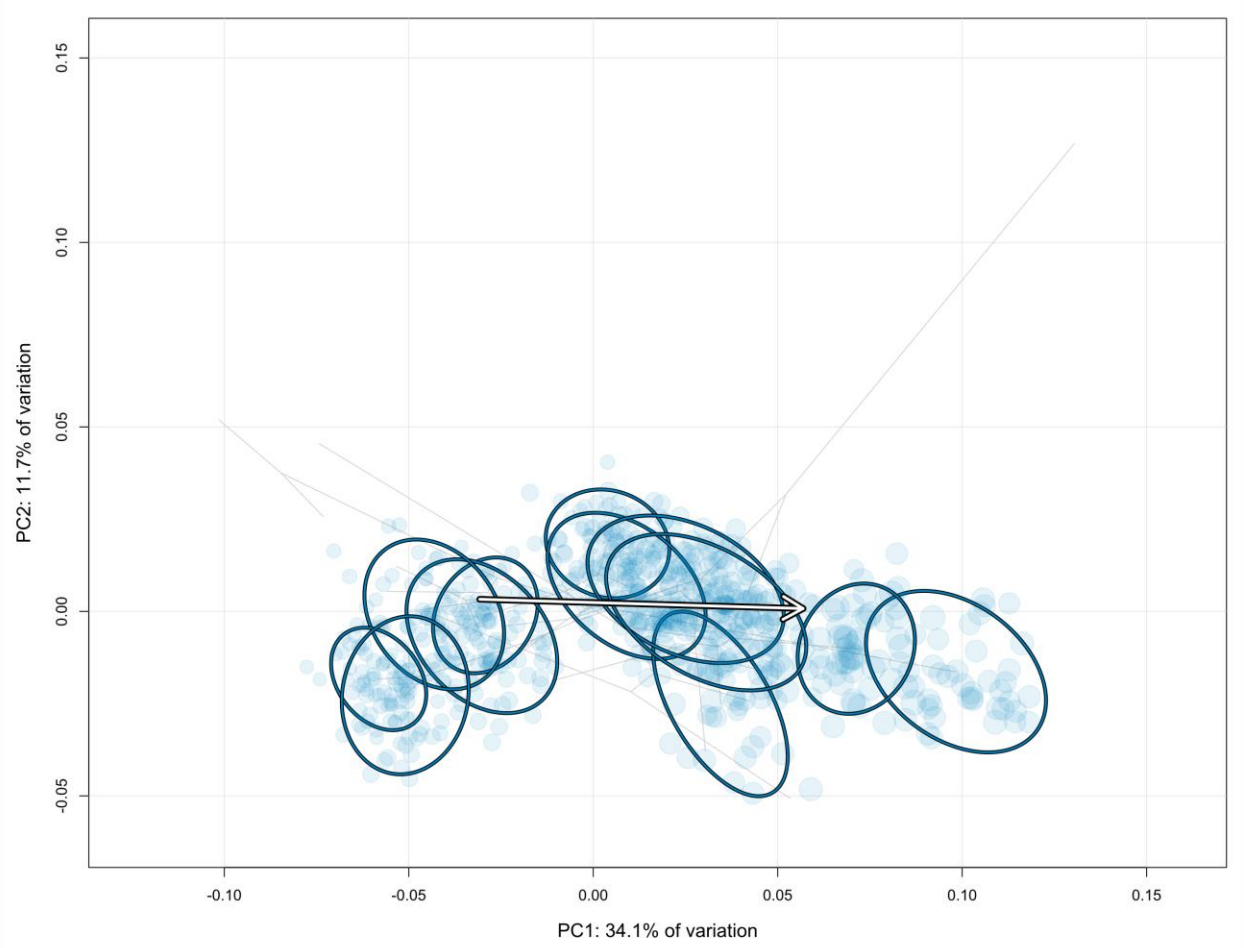

Fig S6.
Interspecific morphospace of Cervidae (similar to Fig 3f), without moose (genus *Alces*). The white arrow is evolutionary allometry, and the blue transparent points are specimens. Ellipses are 95% confidence intervals of each species. Note the congruence between allometry and PC1, and the bias of the ellipses along this axis.

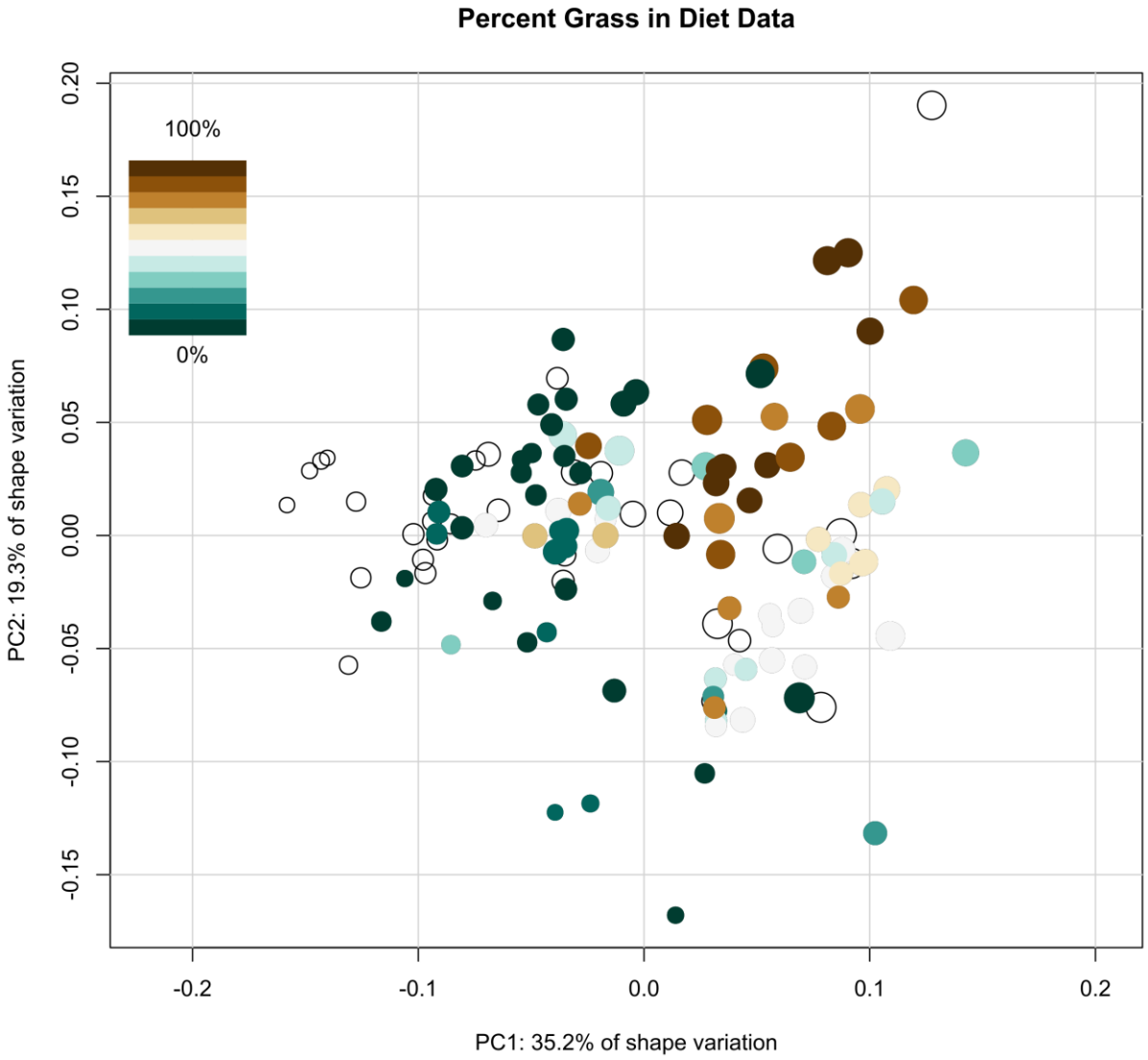

Fig. S7.

Interspecific morphospace with species colored by their % grass in diet value, where exclusive grazers have 100% grass in diet. The uncolored points are species for which these data were unavailable.

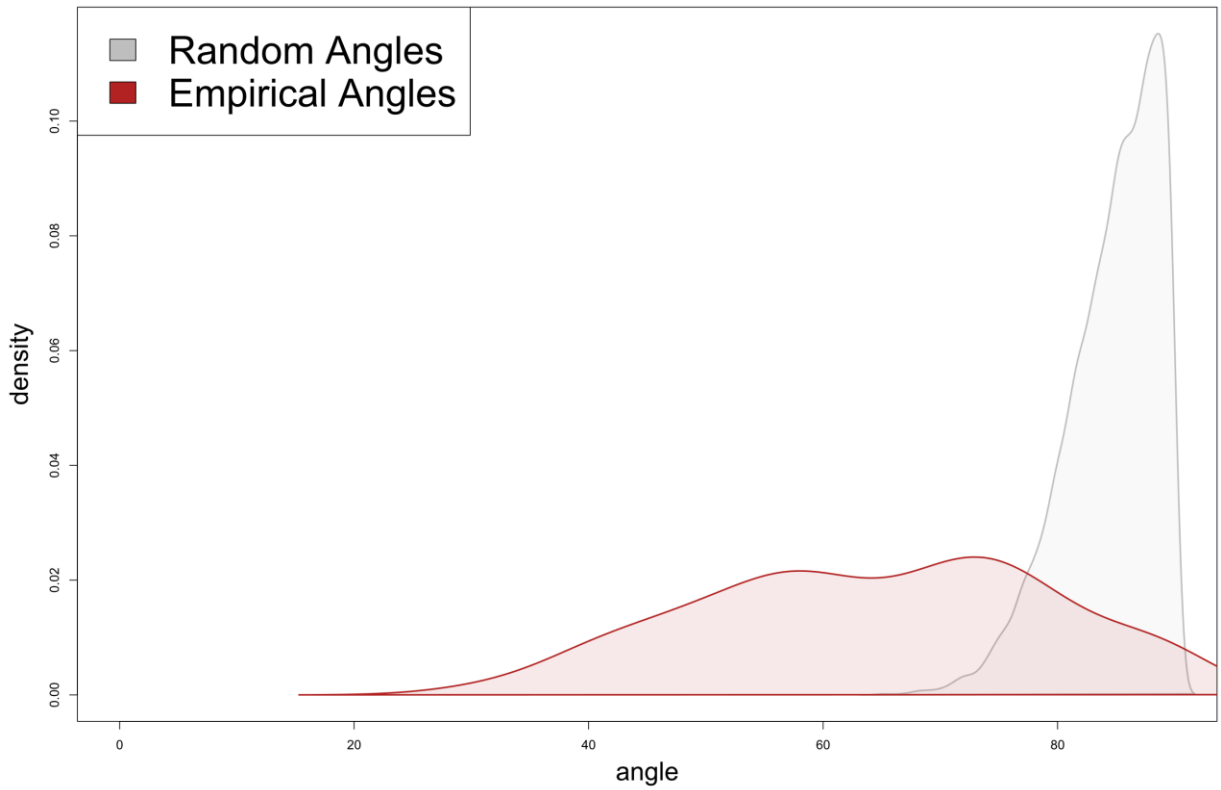

Fig. S8.

Distributions of random angles (gray) of the same dimensionality of our dataset (k=75) and observed angles (red) between the direction of divergence and CREA from our empirical dataset. Note that angles here can have a maximum value of 90 degrees.

Table S1.

Landmark definitions of the geometric morphometrics dataset, from Haber (*22*).

1	Suture junction between the two frontals and the nasals; at the frontal end when there is a gap
2	Suture junction between the two frontals and the parietal; at the frontal end when there is a gap
3	Supraoccipital boss at the dorsal end of the bone
4	Anteroventral suture end of the two palate bones
5	Posteroventral suture end of the two palate bones
6	Meeting point between the two basioccipitals on the foramen magnum rim
7	Meeting point between the two occipitals on the foramen magnum rim
8	Anterior tip of the premaxilla
9	Infraorbital foramen; the most posterior points on the rim from lateral view
10	Anterobuccal edge of the third premolar alveoli; meeting point between the alveoli and the tooth
11	Anterobuccal edge of the first molar alveoli; meeting point between the alveoli and the tooth
12	Anterodorsal suture end between the jugal and the squamosal; at the point where the suture turns in the medial aspect of the zygomatic arch
13	Posteroventral suture end between the jugal and squamosal; at the point where the suture turns into the lateral aspect of the zygomatic arch
14	Suture junction between the parietal, squamosal, and occipital bones
15	Suture junction between the parietal, squamosal, and alisphenoid bones
16	Meeting point between the jugal, frontal, and orbital rims on the postorbital bar
17	Meeting point between the lacrimal, frontal, and orbital rims
18	Meeting point between the lacrimal, jugal, and orbital rims
19	Anterior suture end between the lacrimal and the jugal; at the point where the suture turns dorsally
20	Posterior suture end between the maxilla and the nasal
21	Subnasal meeting point of the maxilla (sometimes premaxilla) and the nasal
22	Anterior tip of the nasal
23	Meeting point between the basioccipital and the foramen magnum condyle
24	Foramen ovale; the most posterior point on the rim
25	Posterobuccal edge of the third molar alveoli; meeting point between the alveoli and the tooth